Boronate Cross-linked ATP- and pH-Responsive Nanogels for Intracellular Delivery of Anticancer Drugs

ARTICLE *in* ADVANCED HEALTHCARE MATERIALS · MARCH 2015

Impact Factor: 5.8 · DOI: 10.1002/adhm.201400550 · Source: PubMed

3 AUTHORS, INCLUDING:

Xuejiao Zhang
Freie Universität Berlin
13 PUBLICATIONS **231** CITATIONS
SEE PROFILE

Katharina Achazi
Freie Universität Berlin
37 PUBLICATIONS **253** CITATIONS
SEE PROFILE

ADVANCED HEALTHCARE MATERIALS

Postfach 10 11 61
69451 Weinheim
Germany
Courier services:
Boschstraße 12
69469 Weinheim
Germany
Tel.: (+49) 6201 606 235
Fax: (+49) 6201 606 500
E-mail: advhealthmat@wiley-vch.de

WILEY-VCH

Dear Author,

Please correct your galley proofs carefully and return them no more than three days after the page proofs have been received.

The editors reserve the right to publish your article without your corrections if the proofs do not arrive in time.

Note that the author is liable for damages arising from incorrect statements, including misprints.

Please note any queries that require your attention. These are indicated with red Qs in the pdf or highlighted as yellow queries in the XML working window.

Please limit corrections to errors already in the text; cost incurred for any further changes or additions will be charged to the author, unless such changes have been agreed upon by the editor.

Reprints may be ordered by filling out the accompanying form.

Return the reprint order form by fax or by e-mail with the corrected proofs, to Wiley-VCH: **advhealthmat@wiley-vch.de**

To avoid commonly occurring errors, please ensure that the following important items are correct in your proofs (please note that once your article is published online, no further corrections can be made):

- **Names** of all authors present and spelled correctly
- **Titles** of authors correct (Prof. or Dr. only: please note, Prof. Dr. is not used in the journals)
- **Addresses** and **postcodes** correct
- **E-mail address** of corresponding author correct (current email address)
- **Funding bodies** included and grant numbers accurate
- **Title** of article OK
- All **figures** included
- **Equations** correct (symbols and sub/superscripts)
- Note: the **resolution of the figures** in the system and the PDF proofs is intentionally of lower quality to avoid slow loading times. Your high-resolution files will be used for the final publication.

Please note: If you send any additional information, such as figures or other display items, to advhealthmat@wiley-vch.de, please also indicate this clearly in the XML working window by inserting a comment using the query tool.

ADVANCED HEALTHCARE MATERIALS

Reprint Order Form 2014
- please return with your proofs -

Editorial Office:

Wiley-VCH Verlag, Boschstrasse 12
69469 Weinheim, Germany

Tel.: (+49) 6201 606 235
Fax: (+49) 6201 606 500

E-mail: advhealthmat@wiley-vch.de
http://www.advhealthmat.de

Manuscript No. _____

Please send me and bill me for

☐ no. of **reprints** via ☐ airmail (+ 25 Euro) ☐ surface mail

☐ no. of **copies of this issue** (1 copy: 25 Euro) via ☐ airmail (+ 25 Euro) ☐ surface mail

☐ **high-resolution PDF file** (330 Euro).

My e-mail address:

_____

Please note: It is not permitted to present the PDF file on the internet or on company homepages

★**Special Offer**★ If you order 200 or more reprints you will get a PDF file for half price.

Information regarding VAT

Please note that from German sales tax point of view, the charge for **Reprints, Issues or Posters** is considered as **"supply of goods"** and therefore, in general, such delivery is a subject to German sales tax. However, this regulation has no impact on customers located outside of the European Union. Deliveries to customers outside the Community are automatically tax-exempt. Deliveries within the Community to institutional customers outside of Germany are exempted from the German tax (VAT) only if the customer provides the supplier with his/her VAT number. The VAT number (value added tax identification number) is a tax registration number used in the countries of the European Union to identify corporate entities doing business there. It starts with a country code (e.g. FR for France, GB for Great Britain) and follows by numbers.

Mail reprints /cover posters / copies of the issue to:

_____
_____
_____
_____
_____

Invoice address:

_____
_____
_____
_____
_____

_____
Date, Signature **Stamp**

VAT no.: _____
(institutes / companies in EU countries only)

Purchase Order No.: _____

Credit Card Payment

VISA, MasterCard, AMERICAN EXPRESS

Please use the Credit Card Token Generator located at the website below to create a token for secure payment. The token will be used instead of your credit card number.

Credit Card Token Generator:
https://www.wiley-vch.de/editorial_production/index.php

Please transfer your token number to the space below.

Credit Card Token Number:

Cover Posters

Posters are available of all the published covers and frontispieces in two sizes

☐ DIN A2 42 x 60 cm / 17 x 24in (one copy: **39 Euro**)
☐ DIN A1 60 x 84 cm / 24 x 33in (one copy: **49 Euro**)

Postage for shipping posters overseas by airmail:
+ 25 Euro

Postage for shipping posters within Europe by surface mail:
+ 15 Euro

Price list for reprints

(The prices include mailing and handling charges. All Wiley-VCH prices are exclusive of VAT)

No. of pages	Price (in Euro) for orders of					
	50 copies	100 copies	150 copies	200 copies	300 copies	500 copies
1-4	345	395	425	445	548	752
5-8	490	573	608	636	784	1077
9-12	640	739	786	824	1016	1396
13-16	780	900	958	1004	1237	1701
17-20	930	1070	1138	1196	1489	2022
for every additional 4 pages	147	169	175	188	231	315

★ **Special Offer** ★ If you order 200 or more reprints you will get a PDF file for half price.

Wiley-VCH Verlag GmbH & Co. KGaA; Location of the Company: Weinheim;
Chairman of the Supervisory Board: Stephen Michael Smith,
Trade Register: Mannheim, HRB 432833, General Partner: John Wiley & Sons GmbH,
Location: Weinheim, Trade Register Mannheim, HRB 432296,
Managing Directors: Bijan Ghawami, Dr. Jon Walmsley

WILEY-VCH

Full Paper

xxxx

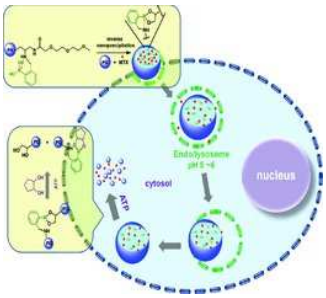

A novel adenosine-5′-triphosphate **(ATP) and pH dual-responsive biodegradable dPG nanogel** are fabricated by inverse nanoprecipitation for the intracellular delivery and release of anticancer drug. The cross-linkers, boronate ester bonds, are cleavable under organelle acidic conditions and the nanogel is further dissociated in response to a high concentration of ATP in the cytoplasm, inducing a complete release of encapsulated drug payload.

ADHM201400550(201400550)

www.MaterialsViews.com

ADVANCED HEALTHCARE MATERIALS
www.advhealthmat.de

Full Paper

Boronate Cross-linked ATP- and pH-Responsive Nanogels for Intracellular Delivery of Anticancer Drugs

Xuejiao Zhang, Katharina Achazi, and Rainer Haag*

Keywords: ATP-responsive, organelle permeation, pH degradation, polyglycerol nanogel

ABSTRACT: A novel adenosine-5′-triphosphate (ATP) and pH dual-responsive degradable nanogel (NG) system are developed based on the complexation of 1,2-diols in dendritic polyglycerol (dPG), and boronic acids, which are conjugated with dPG as the macromolecular cross-linker. The NG is formed by a mild and surfactant-free inverse nanoprecipitation method. An anticancer drug, methotrexate (MTX), is coprecipitated with the macromolecular precursors and cross-linkers to form MTX-loaded NG (NG-MTX) with a loading capacity of 13 wt%. The size of NG is controllable from 100 to 300 nm, which is suitable for the enhanced permeation and retention (EPR) effect and can be degraded into small fragments that are within the clearance limitation in the presence of 5×10^{-3} M ATP or at pH 4 after 24 h. Increasing ATP concentrations and decreasing pH values of the release medium accelerate the release of MTX. Both the real-time cell analysis (RTCA) and MTT results show no cytotoxic effect of NG and a dose-dependent effect of NG-MTX on HeLa cells as well as MCF-7 cells. The fluorescein isothiocyanate (FITC)-labeled NG (FITC-NG) exhibits a time-dependent intracellular uptake tendency and cell organelle permeability as determined by confocal laser scanning microscopy (CLSM) or flow cytometry.

Q1

1. Introduction

Stimuli-responsive carrier systems have been attracted enormous attention in controlled drug delivery due to their robotic response towards intracellular or extracellular stimuli such as pH values, redox conditions, enzymes, temperature, etc.[1] However, single stimuli-responsive systems are often not enough to accomplish a high therapeutic efficacy by themselves. Therefore dual-responsive systems combining two stimuli signals have been recently developed, including pH/redox,[2] pH/magnetic,[3] pH/temperature,[4] temperature/NIR,[5] and enzyme/pH.[6] The combination of adenosine-5′-triphosphate (ATP) and pH-triggered drug delivery system has not yet been reported.

ATP is a multifunctional nucleotide, which plays an important role in cellular metabolism and is considered an essential immunogenic signaling molecule.[7] The intracellular concentration of ATP is in the range of 1×10^{-3} to 10×10^{-3} M, which is much higher than its extracellular concentration.[8] This concentration gradient has been used to trigger the release of guest molecules through the intracellular hydrolysis of ATP into adenosine-5′-diphosphate (ADP), which produce mechanical force to induce the disassembly of the nanocarriers.[9] Kataoka and co-workers[10] also made use of the intra-/extracellular ATP concentration gradient to promote siRNA release from the complexation of siRNA and phenylboronic acid (PBA) by competitively binding ATP with PBA. Moreover, the aptamer–ATP interaction has also been applied to design ATP-responsive systems. The covalent binding of aptamer to carrier scaffold can affect its affinity and selectivity, which is induced by the possible change of the aptamer sequence.[11]

Boronic acids can reversibly form boronate esters with *cis*-1,2- or 1,3-diols, respectively.[12] PBA exhibited equilibrium between uncharged and anionically charged forms in aqueous solution and only the charged PBA can form stable phenylboronate esters. However, the pK_a of PBA is 8.8, which is not beneficial for the formation of stable boronate ester. It has been reported that the introduction of an aminomethyl to the *ortho*-position relative to the boronic acid center can give a dative boron–nitrogen (B–N) interaction, which creates tetrahedral sp^3 boron at or near neutral pH that enhances the binding affinity of boronic acid for diols at neutral pH. This B–N interaction can also decrease the pK_a of corresponding amines,[13] which may help endosomal escape of the carrier system.

Dendritic polyglycerol (dPG) is a highly biocompatible, multifunctional, water-soluble macromolecule that is able to form

X. J. Zhang, Dr. K. Achazi, Prof. R. Haag, Institut für Chemie und Biochemie, Freie Universität Berlin, Takustraße 3, 14195 Berlin, Germany (E-mail: zhangxuejiao1985@gmail.com)
Correspondence to: X. J. Zhang (E-mail: zhangxuejiao1985@gmail.com)

Q2

10.1002/adhm.201400550

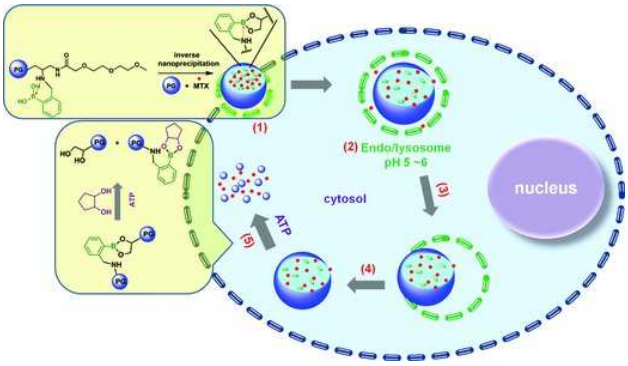

Figure 1. Illustration of intracellular pathway of NG-MTX: 1) Passive targeting and endocytosis of NG, 2) acidity-induced NG swelling and protonation of amino groups, 3) disrupture of organelle membrane, 4) endo/lysosomal membrane permeation, 5) ATP-triggered dissociation of NG.

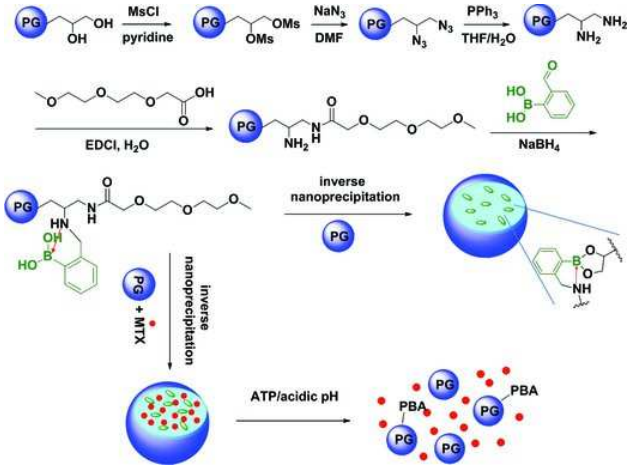

Scheme 1. Synthetic route towards NG and NG-MTX.

boronate ester with PBA due to the existence of 1,2-diol units preferentially located at the periphery of the molecule.[14]

In this study, we presented a new ATP and pH dual-responsive biodegradable dPG nanogel (NG) through inverse nanoprecipitation for the intracellular delivery and release of methotrexate (MTX) in tumor cells (**Figure 1**). It was assumed that the MTX-loaded nanogels (NG-MTX) could enter into the tumor cells by endocytosis thus leading to partial release of MTX in the mildly acidic environment in endo/lysosomal compartments due to the partial cleavage of boronate ester bonds. Under acidic conditions, the swelling of the NG that was induced by the electrostatic repulsion and the partial cleavage of the boronate linkages facilitate the NG breaking up the endo/lysosomal membrane. In the cytoplasm, the NG is further dissociated in response to a high concentration of ATP, which induces a complete release of encapsulated drug payload.

2. Results and Discussion

2.1. NG and NG-MTX Preparation by Inverse Nanoprecipation

The synthetic pathway is shown in **Scheme 1**. dPG was converted into the corresponding dPG-amine (dPGA) with 100% amino functionalities in a three-step process (Supporting Information). Then, 2-[2-(2-methoxyethoxy) ethoxy] acetic acid (PEG-COOH) was conjugated with amine groups by amide coupling in order to introduce PEG moieties and thus reduce the amino amount, which is related to the cytotoxic effect.[15] Furthermore, the macromolecular cross-linker, dPG-Am-PEG-FPBA, was synthesized using a Schiff-base reaction between the amino groups in dPGA and formyl groups in 2-formylphenylboronic acid (FPBA). After being reduced with $NaBH_4$, the dPG-Am-PEG-FPBA conjugate was obtained with *ortho*-amine in the phenyl ring (see red arrow in Scheme 1). The FTIR analysis proved the formation of an amide bond between dPGA and PEG-COOH and the introduction of FPBA to the conjugate. The absorption at 1661 and 1539 cm^{-1} produced the characteristic peaks of amide I and amide II, respectively. The phenyl ring in FPBA was in the region of 1400–1600 cm^{-1}. 1287 and 756 cm^{-1} refer to the vibrations of B-O bonds.[16] In the dried NG, a new band at 1325 cm^{-1} appeared because of the boronate ester formation[17] (Figure S1, Supporting Information).

The ATP and pH dual-responsive NG, composed of dPG as the NG scaffold and dPG-Am-PEG-FPBA as the macromolecular cross-linker, was fabricated by the surfactant-free inverse nanoprecipitation method.[2,18] As depicted in Scheme 1, the NG was formed under mild conditions without any additives, which simplified the purification process. The hydrodynamic diameter of obtained particles is approximately 200 nm determined by dynamic light scattering (DLS) (**Figure 2**A). In Figure 2B, the well-distributed spherical NGs can be observed, the size of which is in accordance with the DLS result. The anticancer drug MTX was coprecipitated with the macromolecular precursors and encapsulated into the NG via an electrostatic interaction between anionic MTX ($pKa = 4.8$ and 5.5) and cationic amino groups in the NG. The MTX-loading capacity was determined by UV–vis to be 13 wt%.

2.2. Degradation of NG

The degradation process was recorded by DLS. As shown in Figure 2C, the size of NG increased due to the swelling of the polymer networks in the first 8 h under the treatment of 5×10^{-3} M ATP. On one hand, ATP could compete with dPG to dissociate the cross-linkers in the NG scaffold, which would reduce the cross-linking degree, resulting in the swelling of the NGs. On the other hand, since the NG was positively charged, the cleavage of the boronate ester could induce an electrostatic repulsion between the charged components.[19] Later on, as more and more boronate esters were cleaved, the NG dissociated into small fragments after 24 h with a similar size as the precursors. The turbidity study also proved the occurrence of degradation of the NGs by adding ATP owing to the increased

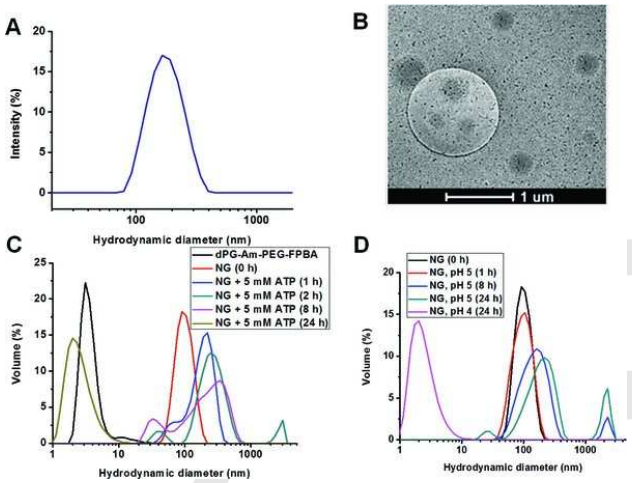

Figure 2. A) Size distribution measured by DLS, B) Cryo-TEM image of NG, degradation profiles of NG C) in the presence of ATP and D) under acidic conditions.

transmittance over time (Figure S2, Supporting Information). Figure 2D shows that the NG only swelled at pH 5 even after 24 h. Further decrease of the pH to 4 caused complete degradation of NG.

2.3. In Vitro Release Study

An ATP and pH cotriggered release of encapsulated drug is desirable, because ATP and pH gradients between intracellular and extracellular environment are both important biological signals. **Figure 3**A shows the release profiles of free MTX and NG-MTX under different ATP concentrations. At pH 7.4, free MTX burst released more than 80% drug in the first 4 h, whereas NG-MTX only released about 40% of the drug after 30 h. Under 0.5×10^{-3} M ATP treatment (mimicking the extracellular ATP concentration), MTX release was not accelerated. However, in 5×10^{-3} M ATP PBS solution (mimicking the intracellular ATP concentration), the release rate of MTX was significantly enhanced, which is in accordance to the NG degradation results.

Figure 3B presents the release profiles of NG-MTX in buffer solutions with different pH values. In the first 4 h, MTX was released faster than the period of 4 to 8 h due to the shorter pathway of MTX on or close to the periphery of the NGs than that of MTX located in the interior of the particle. Moreover, the drug release increased with decreasing pH values of the medium. A reason for this on one hand could be the degradation of boronate ester under acidic conditions. On the other hand, the amines in the NG that protonated at acidic pH could have caused the NG to swell due to electrostatic repulsion, which could facilitate MTX diffusion from the NG.

To mimic the intracellular pathway, the NG-MTX suspension was first immersed in a buffer solution at pH 5 for 3 h to simulate the organelle acidic condition and then transferred into a PBS solution at pH 7.4 with 5×10^{-3} M ATP to simulate the cytosol environment with a higher concentration of ATP.

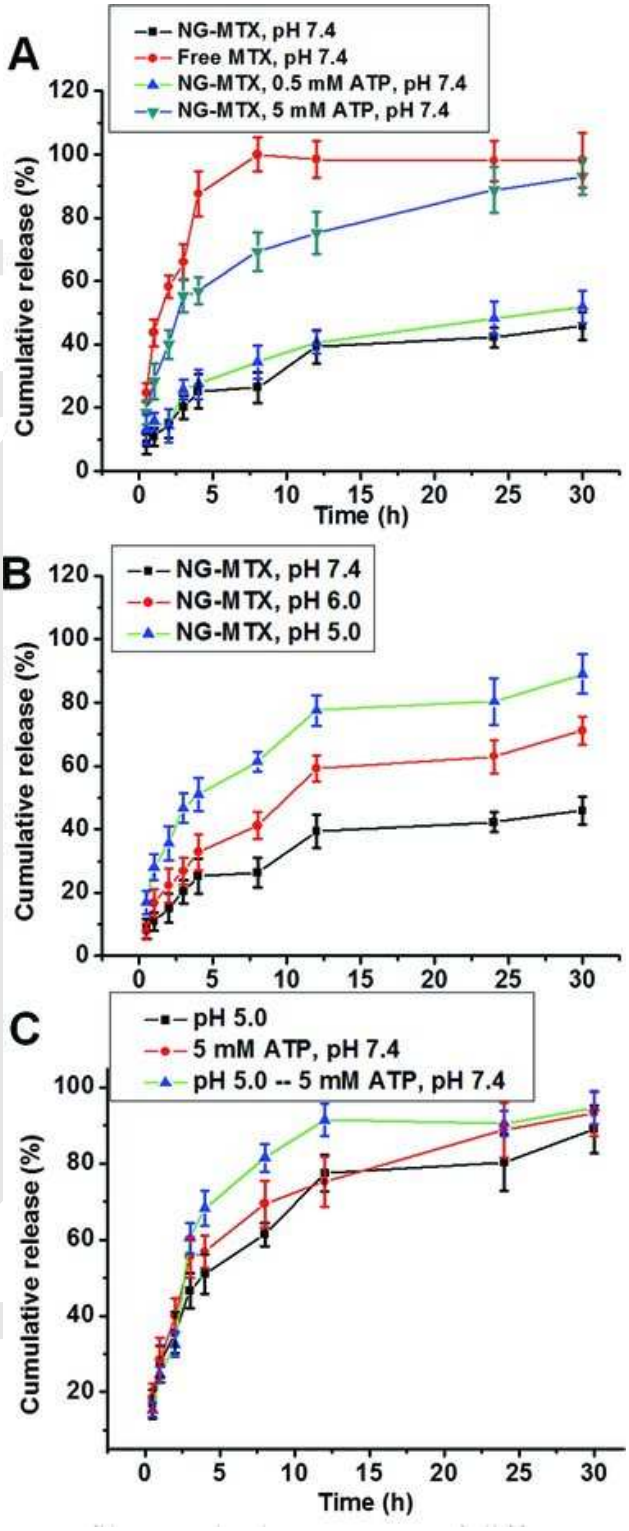

Figure 3. MTX release profiles A) in the presence of different concentrations of ATP, B) in buffers with different pH values, and C) under pH 5 for the first 3 h and then in pH 7.4 buffer with 5×10^{-3} M ATP.

Since the release of MTX could be efficiently triggered by both the acidic condition (pH 5) and the presence of ATP (5×10^{-3} M), no burst effect was observed after it was immobilized in the ATP containing buffer solution (Figure 3C).

2.4. Cellular Toxicity Assessment

An MTT assay was performed to evaluate the cytotoxicity of NG and the antitumor activity of NG-MTX using HeLa cells and MCF-7 cells. NG showed hardly any cytotoxic effects on both HeLa cells and MCF-7 cells up to a concentration of 500 μg mL^{-1} (Figure S3A and S4A, Supporting Information). Cell viability was slightly reduced for the higher concentrations. The dose-response antitumor efficiency was tested by treating HeLa cells and MCF-7 cells with various doses of MTX for 48 h (Figure S3B and S4B, Supporting Information). For both cell lines, NG-MTX exhibited similar or greater cytotoxicity than free MTX. In HeLa cells, NG-MTX displayed a slightly higher cytotoxic effect at concentrations of 32 and 50 μg mL^{-1} than free MTX. It has been reported that MCF-7 cells showed resistance to MTX.[20] NG-MTX more efficiently inhibited cell proliferation than free MTX at concentrations of 75 and 100 μg mL^{-1} (Figure S4B, Supporting Information). The results illustrate that NG-MTX had better antitumor activity for this cell line.

2.5. Real-Time Cell Analysis

MTX is a potent inhibitor of the enzyme dihydrofolate reductase, which plays a key role in the synthesis of DNA precursors and cell growth. Therefore, MTX is a chemotherapeutic agent that mainly inhibits cell proliferation.[21]

The effect of NG, MTX, and NG-MTX on the cell proliferation of HeLa cells and MCF-7 cells was determined online by an xCelligence RTCA device. As shown in **Figure 4**A, **5**A, the NG did not induce any obvious reduction in the cell index (CI) values in all concentrations during the 48 h measurement. Hence, the NG was not toxic toward HeLa cells and MCF-7 cells. Free MTX and NG-MTX displayed a similar cytotoxic behavior towards HeLa cells (Figure 4B,C). However, under 25, 50, and 100 μg mL^{-1} MTX treatment, the CI value decreased in the first 15 h and gradually recovered afterwards. One reason could be the propagation of the remaining cells. Moreover, the efflux of the MTX by HeLa cells could also be an explanation for the CI recovery. As shown in Figure 5B,C, NG-MTX exhibited even higher efficiency in inhibiting the MCF-7 cells. When comparing the IC_{50} value of MTX and NG-MTX for both HeLa cells (Figure 4D) and MCF-7 cells (Figure 5D), in both cases, NG-MTX showed a significant higher efficacy than MTX. The probable reason is that the NG carriers could restrain the multidrug resistance of the tumor cells.

2.6. Intracellular Uptake

The internalization of FITC-labeled NG (FITC-NG) was recorded by CLSM and flow cytometry. As depicted in **Figure 6**, the enhanced green fluorescence observed from 1 to 24 h demonstrates a time-dependent uptake of FITC-NG. After 1 h treatment, the green fluorescence accumulated near the

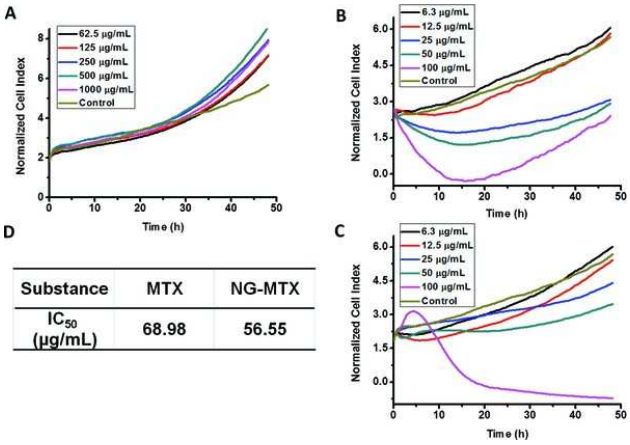

Figure 4. Cytotoxicity profiles of HeLa cells under the treatment of A) NG, B) MTX, and C) NG-MTX; D) IC_{50} values of MTX and NG-MTX against HeLa cells. Cell inhibition was given as a normalized CI recorded over time.

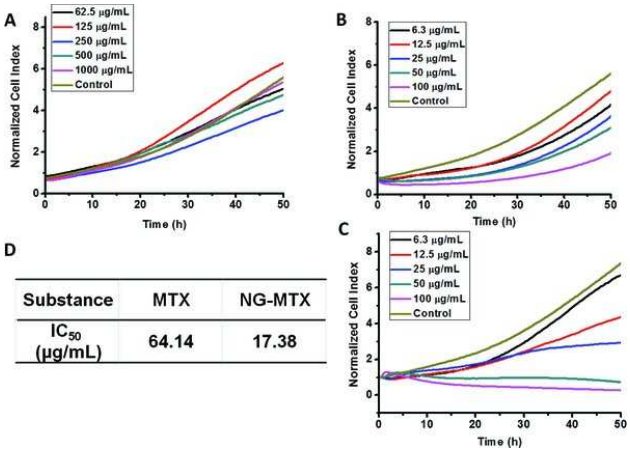

Figure 5. Cytotoxicity profiles of MCF-7 cells under the treatment of A) NG, B) MTX, and C) NG-MTX; D) IC_{50} values of MTX and NG-MTX against MCF-7 cells. Cell inhibition was given as a normalized cell index recorded over time.

cell membrane, demonstrating the attachment of FITC-NG to the cell membrane before endocytosis. After 4 h incubation, the colocalization of the NG (green) and lysosome (red) was observed (yellow), proving that NG entered the cell via an endocytic pathway. The internalization of NG was quantified by flow cytometry. The results are in accordance to the observation by CLSM and show enhanced uptake over time (Figure S6, Supporting Information).

2.7. Endo/Lysosome Membrane Permeation of NG

The aim of this study was to employ the dual-responsivity of boronate ester towards both acidic pH and ATP by utilizing the pH/ATP gradient that exists in the intracellular and extracellular environments to construct a dual-biologically triggered NG

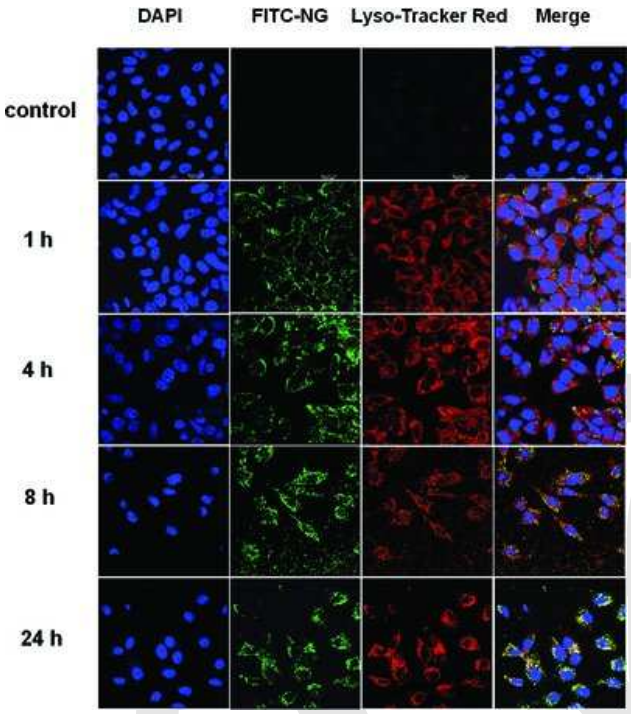

Figure 6. CLSM images of HeLa cells after the treatment of FITC-NG at different time intervals. Lysosome were stained with Lyso-tracker Red (red) and nuclei were stained with DAPI (blue). Green fluorescence represents FITC-NG.

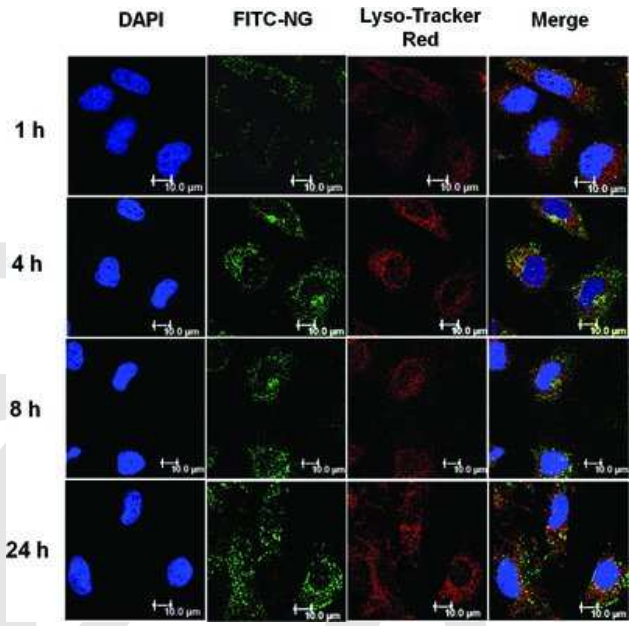

Figure 7. CLSM images of HeLa cells treated with FITC-NG for 1 h, then rinsed thrice with PBS solution and further incubated until 4, 8, and 24 h. The lysosomes were stained with Lyso-tracker Red (red) and the nuclei were stained with DAPI (blue). Green fluorescence: FITC-NG.

delivery vehicle. Therefore, it was very important to monitor the intracellular trafficking of NG. To avoid the constant uptake of the NG after 1 h incubation, the culture medium was replaced by fresh medium without any substance. The cells were further cultured and analyzed by CLSM after predetermined time intervals. The NG and lysosome colocalized after 4 h and the green and red fluorescence separated after 8 h. At 24 h, however, there was not any more colocalization, which demonstrates that the NG permeated the endo/lysosomal membrane and reached the cytosol (**Figure 7**). There are two possible explanations for this. On the one hand, the B–N interaction could have decreased the pK_a of the secondary amine, which would have encouraged the NG to protonate after endocytosis and thus facilitated the permeation of acidic organelle membrane, whereby the pH titration proved that the zeta potential increased with decreasing pH values (Figure S7, Supporting Information). On the other hand, since the NG was positively charged, the acidic pH could have induced the NG to swell because of the electrostatic repulsion and partial cleavage of the boronate ester bond (Figure 2D). Moreover, it has been reported that the swelling of NG can disrupt the lysosome membrane.[21]

3. Conclusion

In this study, a new ATP and pH dual-responsive degradable NG has been designed. It is synthesized by cross-linking with boronate ester bonds between 1,2-diols in dPG and boronic acid in FPBA for the intracellular delivery of anticancer drugs. MTX was encapsulated by electrostatic interactions and can be rapidly released upon treatment with ATP and acidic pH conditions. The NG could swell under organelle pH conditions, which facilitated the permeation of organelle membrane. Furthermore, in the presence of a cytosolic ATP concentration, the NG could degrade and release the drug payload in the cytosol. This new approach allows for a well-defined release of encapsulated drugs and showed higher efficacy than the free MTX.

4. Experimental Section

Materials: dPG ($\overline{M}_w$= 5.8 kDa, $\overline{M}_w$= 7.5 kDa, PDI = 1.29) was prepared based on a published procedure.[22] FPBA, 2-[2-(2-methoxyethoxy) ethoxy] acetic acid (PEG-COOH), fluorescein isothiocyanate (FITC), 1-ethyl-3-(3-dimethylaminopropyl)carbodiimide (EDCI), and MTX were purchased from Sigma–Aldrich (Germany). 4′6-diamidino-2-phenylindole (DAPI) and LysoTracker Red DND-99 were purchased from Lifetechnology (Germany). All other chemicals were obtained from Acros (Germany) or Fluka (Germany). For cell culture experiments, HeLa cells (DSMZ no.: ACC 57) cultured in RPMI supplemented with 10% fetal calf serum and 1 $\times$ 10^{-3} M sodium pyruvate and MCF-7 cells (DSMZ no.: 115) cultured in RPMI supplemented with 10% fetal calf serum,

MEM nonessential amino acids, 1×10^{-3} M sodium pyruvate, and 10 μg mL^{-1} human insulin.

Characterization: ^{1}H NMR spectra were recorded on a Bruker ECX 400 operating at 400 MHz by using the residual-deuterated solvent peaks as internal standard. IR measurements were carried out on a Nicolet AVATAR 320 FT-IR 5 SXC that was equipped with a DTGS detector from 4000 to 600 cm^{-1}. The DLS measurements were carried out at 25 °C using a Zetasizer Nano-ZS from Malvern Instruments equipped with a 633-nm He–Ne laser. The UV measurements of MTX were performed at 372 nm. The morphology of NGs was observed using cryogenic transmission electron microscopy (Cryo-TEM, Philips Tecnai F20 FEG).

Synthesis of dPG-Am-PEG: Fully functionalized dPGA was synthesized by a previously reported three-step procedure.[23] Briefly, OH groups were transformed into mesyl (Ms) groups followed by the conversion of Ms groups into azide (N_3) moieties, and finally primary amino (NH_2) functionalities were obtained by the reduction of N_3 using triphenylphosphine as a reducing agent. Then PEG-COOH was conjugated to dPGA by amide coupling. PEG-COOH (1.01 mL, 8 mmol) was dissolved in 10 mL milli-Q-water and the solution was cooled to 0 °C, followed by the addition of EDCI (4.26 g, 27.4 mmol). After 0.5 h, dPGA (1 g, 0.175 mmol) was dissolved in 10 mL milli-Q-water and slowly added to the above solution. The mixture was stirred overnight at ambient temperature under argon atmosphere. After dialysis against distilled water (molecular weight cut-off 2000 g mol^{-1}), the pure compound (PEG-COOH functionality 51.3%, conversion 85.5%, yield 82%) was obtained by lyophilization. ^{1}H NMR (400 MHz, D_2O, 25 °C): δ = 2.25–3.12 (–CH_2–NH$_2$ or –CH–NH$_2$), 3.20–3.84 (dPG backbone or PEG-COOH backbone), 4.03 (2H, –NH–CO–CH_2–).

Synthesis of dPG-Am-PEG-FPBA Conjugates: FPBA (57.8 mg, 0.386 mmol) was dissolved in 20 mL methanol together with dPG-Am-PEG (1 g, 0.082 mmol) and the mixture was stirred overnight at room temperature under argon atmosphere. The mixture turned dark yellow. Then, three equivalents $NaBH_4$ (43.8 mg, 1.158 mmol) were added to reduce the imine bond and the solution turned light yellow. The product was purified by dialyzing it against distilled water (molecular weight cut-off 2000 g mol^{-1}) and the final conjugate (FPBA functionality 5%, conversion 83.3%, yield 79.2%) was light yellow after lyophilization. FITC-labeled dPG-Am-PEG-FPBA was generated by reacting FITC with amines. ^{1}H NMR (D_2O, 400 MHz): δ = 7.07–7.51 (4H, ArH), 3.90 (2H, ArH–CH_2–NH).[12a]

Synthesis of NG by Inverse Nanoprecipitation: 1 mL dPG-Am-PEG-FPBA (10 mg mL^{-1}) and 4 mL dPG (10 mg mL^{-1}) aqueous solutions were mixed and immediately injected into 200 mL acetone in a 500-mL round-bottom flask with intensive stirring. Once the mixture was homogeneous, the stirring was stopped and the in situ gelation was performed at room temperature for 24 h. The pure NG was obtained by evaporating acetone and dialyzing against distilled water (molecular weight cut-off 2000 g mol^{-1}), followed by lyophilization. FITC-NGs were fabricated by mixing FITC-labeled dPG-Am-PEG-FPBA and dPG following the same procedure.

NG-MTX Preparation: To prepare NG-MTX, 1 mL MTX solution (20 mg mL^{-1}) in water was added to the mixture of 1 mL dPG-Am-PEG-FPBA (10 mg mL^{-1}) and 4 mL dPG (10 mg mL^{-1}) aqueous solution. The 6 mL solution was rapidly injected into 240 mL acetone in a round-bottom flask under intensive stirring. The system was kept immobile for 24 h, and then acetone was evaporated. To remove the unloaded MTX small molecules, a combined ultrafiltration and centrifugation technique (Amicon Ultra filter, Millipore, 10 kDa MWCO) was applied. NG-MTX was obtained by lyophilization and the loading capacity was detected by UV–vis at 372 nm.

ATP/pH-Triggered Degradation of NG: 10 mg NG was homogeneously suspended in different 10 mL solutions, respectively. The suspensions were kept at 37 °C in a water bath with continuous stirring. DLS measurements were performed at predetermined time points.

In Vitro Drug Release: 500 μL NG-MTX suspension (10 mg mL^{-1}) in phosphate buffer saline (PBS, pH 7.4) was transformed to a dialysis tube (molecular weight cut-off 2000 g mol^{-1}) and immersed in 25 mL of different medium solutions at 37 °C under continuous stirring (200 rpm). 1 mL of the release medium outside the dialysis tube was taken out at predetermined time intervals and a complementary volume of fresh medium was added. The quantification of MTX was carried out by UV–vis spectrophotometer at λ = 372 nm. All the release experiments were carried out in triplicate, and the results were reported as mean ± standard deviation.

Cellular Toxicity of NG and NG-MTX: MTT cell viability assay was used to evaluate the cytotoxicity of the NG. HeLa (DSMZ no.: ACC 57) and MCF-7 (DSMZ no.: ACC 115) cells were seeded into 96-well plates at a concentration of 5000 per well and incubated for 24 h. Then the culture medium was removed and 100 μL of NG suspensions diluted in cell culture medium in different concentrations was added. Untreated cells were used as control. After 48 h incubation, 10 μL of MTT solution (5 mg mL^{-1} in PBS) was added into each well and further incubated for 2 h. Then the culture medium was carefully removed and 100 μL of DMSO was added into each well. After the purple formazan crystals completely dissolved, a microplate reader measured the absorbance at 570 nm. The experiment was repeated for three times and the mean values were reported.

Real-Time Cell Analysis (RTCA): The RTCA assay is a real-time technique to dynamically monitor the cell viability. Microelectrode-coupled microtiter plates were used to culture the cells, and the cell number, cell morphology, and degree of cell adhesion were reflected by the electrode impedance.[24] The untreated cells attach to the bottom of the well and cause an increase in the CI value due to the increased impedance. When treated with a toxic compound, the cells die and detach from the bottom, displaying a decrease of the CI value. 50 μL of culture medium was added to each well of the E-plate 96 (Roche, Mannheim, Germany) for background measurements. HeLa or MCF-7 cells were then added at a concentration of 3000 or 5000 cells per well, respectively, for 24 h incubation, which was followed by adding NG or NG-MTX suspensions diluted in culture medium at different concentrations. Untreated cells were used as control. The E-plate was incubated and monitored on the RTCA SP system (Roche) for 48 h in time intervals of 15 min. Analysis was performed by using the RTCA software

version 1.2.1. Four replicates were measured for each sample and the mean values were reported.

Cellular Uptake by Confocal Laser Scanning Microscopy: HeLa cells were used to examine the intracellular uptake of FITC-NG. HeLa cells were seeded in a 24-well plate at 1×10^5 cells per well. After 24 h, the medium was replaced with 1 mL of fresh medium containing FITC-NG (100 μg mL^{-1}). After 1, 4, 8, or 24 h incubation, the culture medium was removed and the cells were rinsed three times with PBS solution. The cells were stained with LysoTracker Red DND-99 (Invitrogen, Germany) for 30 min followed by rinsing thrice with PBS. After the cells were fixed with 4% paraformaldehyde PBS solution, the cell nuclei were stained with DAPI (Invitrogen, Germany) for 30 min, followed by dryness. To track the pathway of the NGs, the cells were rinsed with PBS solution after 1 h incubation in the FITC-NG containing culture medium and stained at predetermined time intervals (1, 4, 8, and 24 h). The cells were observed with a CLSM (Leica, Germany) and analyzed using the Leica 2.6.0 software.

Flow Cytometry: HeLa cells were cultured in a 24-well plate at 5×10^5 cells per well for 24 h and then treated with FITC-NG containing culture medium at a concentration of 100 μg mL^{-1}. After 1, 4, 8, or 24 h incubation, the culture medium was removed and the cells were rinsed thrice with PBS and harvested with trypsin. Cells were fixed with 4% paraformaldehyde solution and resuspended in PBS supplemented with 1% fetal calf serum and 0.1% sodium azide. The quantification of fluorescence was done with a FACScalibur (Becton Dickinson, Heidelberg, Germany).

Supporting Information

Supporting Information is available from the Wiley Online Library or from the author.

Acknowledgements

The authors thank Dr. Christoph Böttcher for the cyro-TEM measurements, Dr. Florian Paulus for the PG synthesis and Dr. Pamela Winchester for proofreading this manuscript. This study was supported by the Chinese Scholar Council (CSC), the focus area nanoscale of Freie Universität Berlin (www.nanoscale.fu-berlin.de), and the core-facility biosupramol (www.biosupramol.de).

Received: September 1, 2014
Revised: October 8, 2014
Published Online: MM DD, YYYY

[1] a)S. Mura, J. Nicolas, P. Couvreur, *Nat. Mater.* **2013**, *12*, 991; b)J. Xu, S. Luo, W. Shi, S. Liu, *Langmuir* **2005**, *22*, 989; c)Z. Ge, S. Liu, *Chem. Soc. Rev.* **2013**, *42*, 7289; d)J. Hu, S. Liu, *Acc. Chem. Res.* **2014**, *47*, 2084; e)S. Choi, A. Tripathi, D. Singh, *J. Biomed. Nanotechnol.* **2014**, *10*, 3162.

[2] X. Zhang, K. Achazi, D. Steinhilber, F. Kratz, J. Dernedde, R. Haag, *J. Controlled Release* **2014**, *174*, 209.

[3] W. Wu, J. Shen, Z. Gai, K. Hong, P. Banerjee, S. Zhou, *Biomaterials* **2011**, *32*, 9876.

[4] a)Y. Shen, X. Ma, B. Zhang, Z. Zhou, Q. Sun, E. Jin, M. Sui, J. Tang, J. Wang, M. Fan, *Chem. Eur. J.* **2011**, *17*, 5319; b)T. Zhou, C. Xiao, J. Fan, S. Chen, J. Shen, W. Wu, S. Zhou, *Acta Biomater.* **2013**, *9*, 4546; c)J. Peng, T. Qi, J. Liao, M. Fan, F. Luo, H. Li, Z. Qian, *Nanoscale* **2012**, *4*, 2694.

[5] H. Wang, F. Ke, A. Mararenko, Z. Wei, P. Banerjee, S. Zhou, *Nanoscale* **2014**, *6*, 7443.

[6] L. Dong, S. Xia, KeWu, Z. Huang, H. Chen, J. Chen, J. Zhang, *Biomaterials* **2010**, *31*, 6309.

[7] Y. W. Noh, S. H. Kong, D. Y. Choi, H. S. Park, H. K. Yang, H. J. Lee, H. C. Kim, K. W. Kang, M. H. Sung, Y. T. Lim, *ACS Nano* **2012**, *6*, 7820.

[8] a)M. W. Gorman, E. O. Feigl, C. W. Buffington, *Clin. Chem.* **2007**, *53*, 2318; b)F. M. Gribble, G. Loussouarn, S. J. Tucker, C. Zhao, C. G. Nichols, F. M. Ashcroft, *J. Biol. Chem.* **2000**, *275*, 30046.

[9] S. Biswas, K. Kinbara, T. Niwa, H. Taguchi, N. Ishii, S. Watanabe, K. Miyata, K. Kataoka, T. Aida, *Nat. Chem.* **2013**, *5*, 613.

[10] M. Naito, T. Ishii, A. Matsumoto, K. Miyata, Y. Miyahara, K. Kataoka, *Angew. Chem. Int. Ed.* **2012**, *51*, 10751.

[11] X. He, Y. Zhao, D. He, K. Wang, F. Xu, J. Tang, *Langmuir* **2012**, *28*, 12909.

[12] a)M. Piest, M. Ankoné, J. F. J. Engbersen, *J. Controlled Release* **2013**, *169*, 266; b)J. Ren, Y. Zhang, J. Zhang, H. Gao, G. Liu, R. Ma, Y. An, D. Kong, L. Shi, *Biomacromolecules* **2013**, *14*, 3434; c)X. Wu, Z. Li, X. X. Chen, J. S. Fossey, T. D. James, Y. B. Jiang, *Chem. Soc. Rev.* **2013**, *42*, 8032; d)Y. Kotsuchibashi, R. V. C. Agustin, J. Y. Lu, D. G. Hall, R. Narain, *ACS Macro Lett.* **2013**, *2*, 260.

[13] S. L. Wiskur, J. J. Lavigne, H. Ait-Haddou, V. Lynch, Y. H. Chiu, J. W. Canary, E. V. Anslyn, *Org. Lett.* **2001**, *3*, 1311.

[14] M. Calderón, M. A. Quadir, S. K. Sharma, R. Haag, *Adv. Mater.* **2010**, *22*, 190.

[15] H. Greim, D. Bury, H.-J. Klimisch, M. Oeben-Negele, K. Ziegler-Skylakakis, *Chemosphere* **1998**, *36*, 271.

[16] X. Zou, D. Liu, L. Zhong, B. Yang, Y. Lou, Y. Yin, *Carbohydr. Polym.* **2012**, *90*, 799.

[17] J. Xu, D. Yang, W. Li, Y. Gao, H. Chen, H. Li, *Polymer* **2011**, *52*, 4268.

[18] D. Steinhilber, M. Witting, X. Zhang, M. Staegemann, F. Paulus, W. Friess, S. Küchler, R. Haag, *J. Controlled Release* **2013**, *169*, 289.

[19] R. B. K. C., P. Xu, *Adv. Mater.* **2012**, *24*, 6479.

[20] D. R. Nogueira, L. Tavano, M. Mitjans, L. Pérez, M. R. Infante, M. P. Vinardell, *Biomaterials* **2013**, *34*, 2758.

[21] S. A. Yoon, J. R. Choi, J. O. Kim, J. Y. Shin, X. Zhang, J. H. Kang, *Cancer Res. Treat.* **2010**, *42*, 163.

[22] D. Gröger, F. Paulus, K. Licha, P. Welker, M. Weinhart, C. Holzhausen, L. Mundhenk, A. D. Gruber, U. Abram, R. Haag, *Bioconjugate Chem.* **2013**, *24*, 1507.

[23] S. Rolle, H. Zhou, R. Haag, *Mol. Diversity* **2005**, *9*, 305.

[24] a)A. B. Ryder, Y. Huang, H. Li, M. Zheng, X. Wang, C. W. Stratton, X. Xu, Y. W. Tang, *J. Clin. Microbiol.* **2010**, *48*, 4129; b)J. M. Atienza, J. Zhu, X. Wang, Y. Abassi, *J. Biomol. Screen* **2005**, *10*, 795; c)K. Solly, X. Wang, X. Xu, B. Strulovici, W. Zheng, *Assay Drug Dev. Technol.* **2004**, *2*, 363; d)J. Z. Xing, L. Zhu, J. A. Jackson, S. Gabos, X. J. Sun, X. B. Wang, X. Xu, *Chem. Res. Toxicol.* **2005**, *18*, 154.

Q1 **PROD to AU: Author: Please define MTT in abstract as well as in text.**

Q2 **PROD to AU: Author: Please provide the highest academic title (Dr.Prof.) for Xuejiao Zhang, where applicable.**

Q3 **PROD to AU: Please check the appearance of KeWu in ref. X**

Q4 **PROD to AU: Please check the appearance of R. B. K. C. in ref. X**